Integrated Hydrogeochemical Groundwater Flow Path Modelling in an Arid Environment

Milad Masoud [1,4,*], Natarajan Rajmohan [1], Jalal Basahi [2], Michael Schneider [3], Burhan Niyazi [2] and Abdulaziz Alqarawy [1,2]

1   Water Research Center, King Abdulaziz University, Jeddah 21598, Saudi Arabia
2   Department of Hydrology, Faculty of Meteorology, Environment and Arid Land Agriculture, King Abdulaziz University, Jeddah 21598, Saudi Arabia
3   Hydrogeology Group, Institute of Geological Sciences, Freie Universitaet, 14195 Berlin, Germany
4   Hydrology Department, Desert Research Centre, Cairo 11753, Egypt
*   Correspondence: mhmasoud@kau.edu.sa

Abstract: In this study, water-rock interaction, salinity sources, evolution, and the mixing of groundwater were modelled. The objectives of this research are to understand the hydrogeochemical factors that govern groundwater composition in a shallow aquifer system, Jazan Province, Saudi Arabia. The study aquifer is called a Quaternary aquifer, which is composed of gravel, sand, sandstone, and intercalated with some shale. In this study, 80 groundwater samples have been collected and analyzed for major ions and 30 representative samples were analyzed for Oxygen-18 ($\delta^{18}O$) and Deuterium (δD). NETPATH and environmental isotopes were integrated and applied to study the overall geochemical processes and to identify the salinity source in the groundwater. Saturation indices calculated for carbonates minerals indicates that 49%, 74%, and 61% of groundwater samples are undersaturated in terms of calcite, aragonite, and dolomite minerals, respectively. The remaining groundwater samples (51%, 39%, and 26%) are close to saturation with calcite, dolomite, and aragonite minerals, respectively. The saturation indices of gypsum, anhydrite, silica, strontionite, and sepiolite minerals show undersaturation in all groundwater samples, which is likely due to the dilution through the groundwater recharge from the surface runoff. In this study, water-rock interaction models were employed with the concentration of major ions of all selected groundwater samples, in addition to reference waters such as rain and sea waters, to evaluate the chemistry of groundwater in the flow path. Mixing calculations suggested that there is a variable contribution of rainwater (5% to 53%) in groundwater samples. The results indicate that evaporation and infiltration have a major impact on water chemistry in the study site. The intrusion of seawater at the coastal zone is well identified in some wells. Stable isotope data ($\delta^{18}O$ and δD) support the results and underline the impact of evaporation processes on the groundwater and infiltration of evaporated water.

Keywords: groundwater hydrochemistry; flow path modelling; mixing calculation; evaporation; stable isotopes; Saudi Arabia

1. Introduction

Processes of water-rock interaction are controlling the physico-chemical alterations in water-bearing formations and accordingly produce dissolved ions in groundwater [1–7]. The resulted concentration of the main solutes of groundwater is controlled by the characteristics of the original rainwater chemistry, the geologic situation of the aquifer, and the extension of the water-rock reaction behavior. Earlier studies [8–12] also reported that along the groundwater flow path from the recharge to the discharge area, complex chemical reactions are occurring, namely, dissolutions/precipitations, ion exchange, and redox reaction processes. All these chemical reactions, which often take place simultaneously, could be forecasted through hydrogeochemical modeling and with extra accuracy by the

flow pathway modeling of water-rock interaction. Geochemical modeling is a well-known and important tool that is used in several studies. Reference [13] studied soil chemistry using a geographic information system (GIS) based on the geostatistical module and physiographic features of the soil. Reference [14] studied groundwater quality deterioration by the integration of GIS and field investigation. El-Zeiny et al. [15] studied heavy metals in soil and dust based on geospatial and statistical analyses using satellite images.

Different studies have been conducted in the Kingdom of Saudi Arabia (KSA) to assess and evaluate groundwater quality and characteristics [16–21]. Only a few studies, however, have focused on the geochemical models of groundwater; hence, this research is very important to implement in the study area.

NETPATH is one of the geochemical modeling tools and is considered a valuable method to predict the processes of dissolution and the precipitations of minerals between the water and the water-bearing formations during groundwater movement [22,23]. According to Trabelsi and Zouari [24], the geochemical model is a very important tool to study and understand the groundwater salinity source and the drawdown of groundwater level, which is important for water resources management with a view to sustainable development and optimizing management strategies. Reference [25] was the first researcher who reported on the theory of implementation of geochemical models to natural groundwater systems.

It should be also noted that the selection of the initials or endmember waters depended on the fact that they are thought to be potential sources that can affect the chemical compositions of groundwater in the final waters. In other words, the groundwater from these endmember waters can be identified through their chemical compositions, based on the fact that they are primarily controlled by water-rock interactions in the absence of groundwater mixing [26]. The endmember mixing analysis based on tracers is a technique for determining the proportion of sources in mixed water according to the mass conservation law [27–29].

The geochemical characteristics of groundwater depend on the recharge sources and the subsurface geochemical processes throughout the water-bearing formation, namely atmospheric (meteoric), fossil, or marine water, in addition to the water-bearing formation reactions [30–32]. These factors are controlling the water quality as it flows from the recharge to discharge areas. Magnitudes of such variations depend on the physico-chemical characteristics of the adjacent geologic formations, sedimentation processes, water temperature, groundwater flow velocity, and climate changes.

This research aims to study the salinity source of groundwater, to study the geochemical evolution, and to understand and explain the hydro-chemical factors governing the groundwater quality in the flow pathways in a shallow groundwater system, Jazan Province, Saudi Arabia, using groundwater flow path modelling.

2. Study Area

The KSA is one of the arid countries, which is characterized by an arid to hyper-arid climate in most of its area, except in some parts which are characterized by a semi-arid to semi-humid climate, especially in the southwest part of the country. The study area, Jazan Province, is located in the south-western part of KSA. The study area represents one of the most important areas in the KSA in terms of renewable water resources because it receives a considerable amount of rainfall, which recharges the shallow groundwater in the study area. The study area is located between longitudinal 41°34′ and 43°34′ E and latitudinal 16°15′ and 18°22′ N with a hydrological area (watershed) of about 24,215 km^2, while the administration area of Jazan Province has an extension of 15,000 km^2 (Figure 1). The study area is characterized by semi-arid climatic features where the mean annual precipitation (56 years, 1960–2015) ranges from 120 to 400 mm. The rainy seasons are in summer through the Indian monsoon season (between April and September) and in winter through Mediterranean climate conditions.
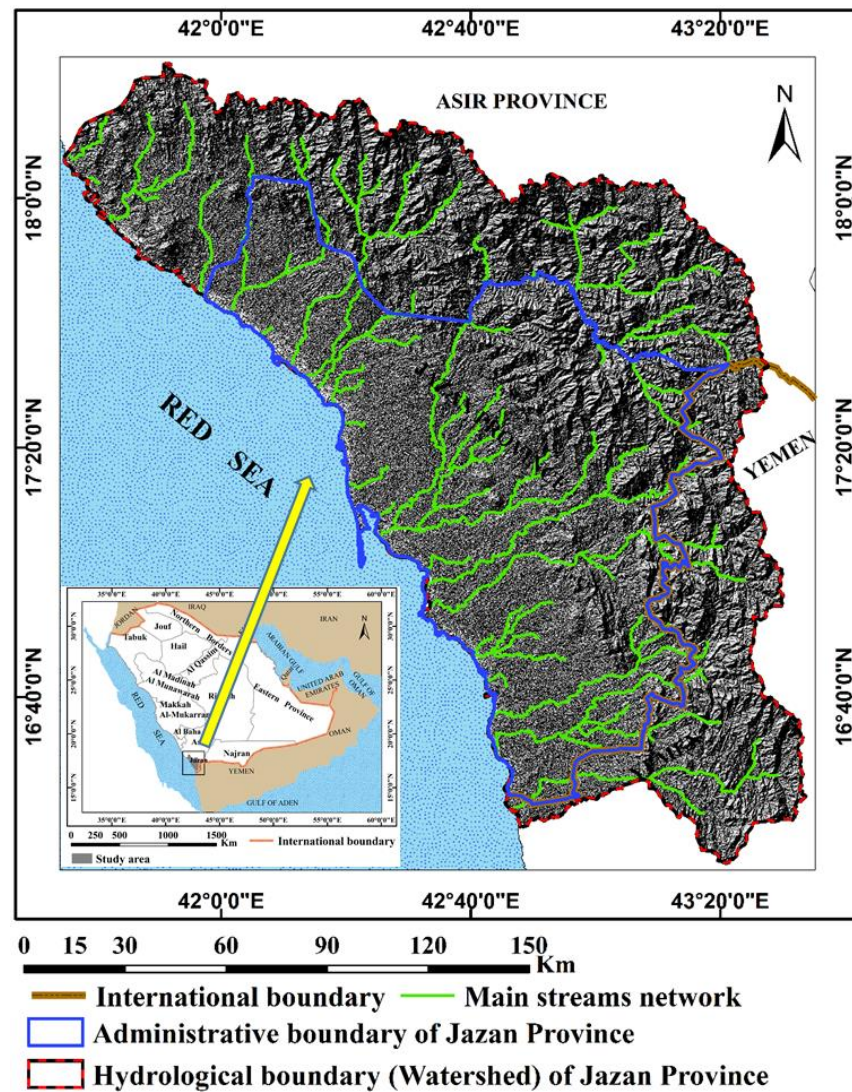
Figure 1. Location map of the study area.

From a geomorphological point of view, the study area represents the western part of the Asir mountainous range, which has a topographic elevation of up to 2980 m amsl with a very steep slope at the escarpment. The drainage basins are initiated from the upstream portion (high elevated portions) and discharges the water to the western direction (Red Sea), as shown in Figure 2. The flood plains, where the main streams are filled by alluvial wadi deposits, are considered to be the main portion of the shallow Quaternary unconfined aquifer of the study area.
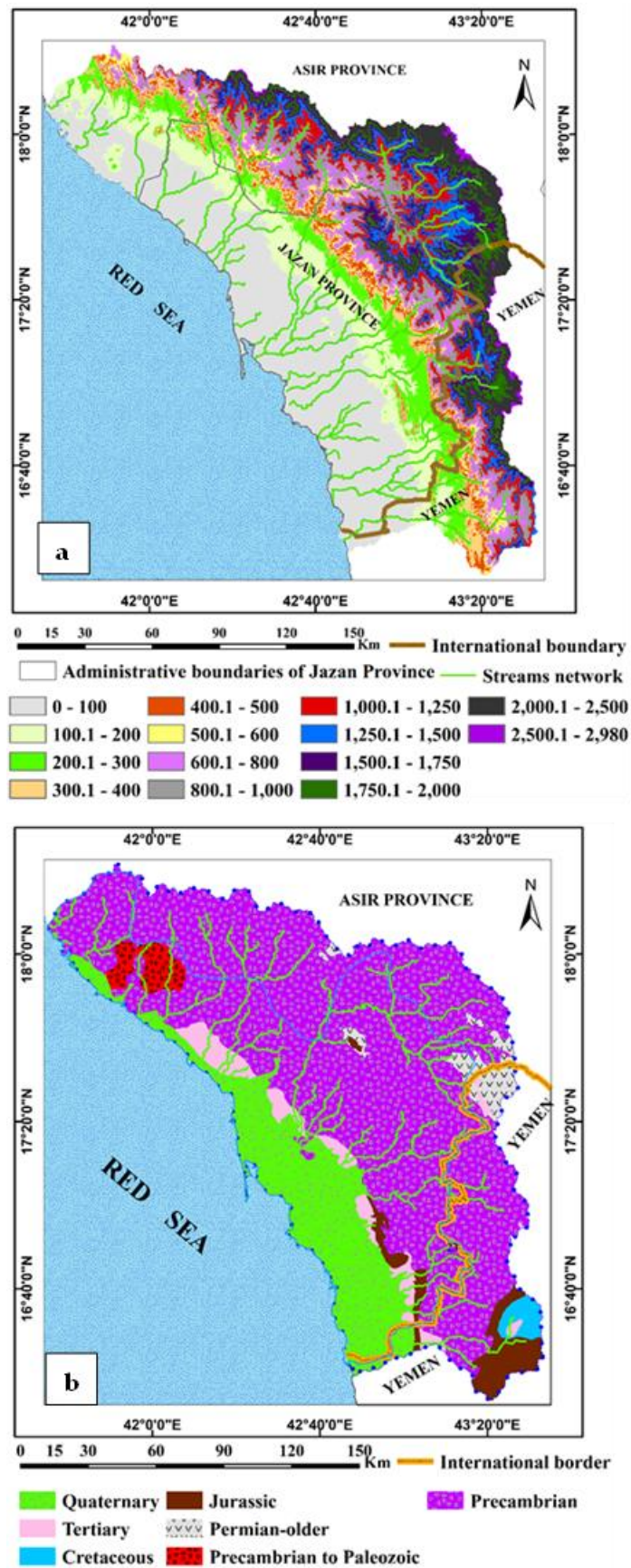
Figure 2. Digital elevation map (**a**) and geological map (**b**).

Geologically, the area of study represents an important portion of the Arabian Shield, which is composed of Precambrian Plutonic igneous and metamorphic rocks. In addition to the Precambrian rocks, the study area is composed of a wide range of geologic formations from Precambrian to recent (Figure 2). The shallow aquifer, whose water resources are being recharged, is composed of a considerable thickness of Quaternary deposits comprising conglomerates, gravels, sands, sandstone, and shale, as shown in the hydrogeological cross-sections (Figure 3).
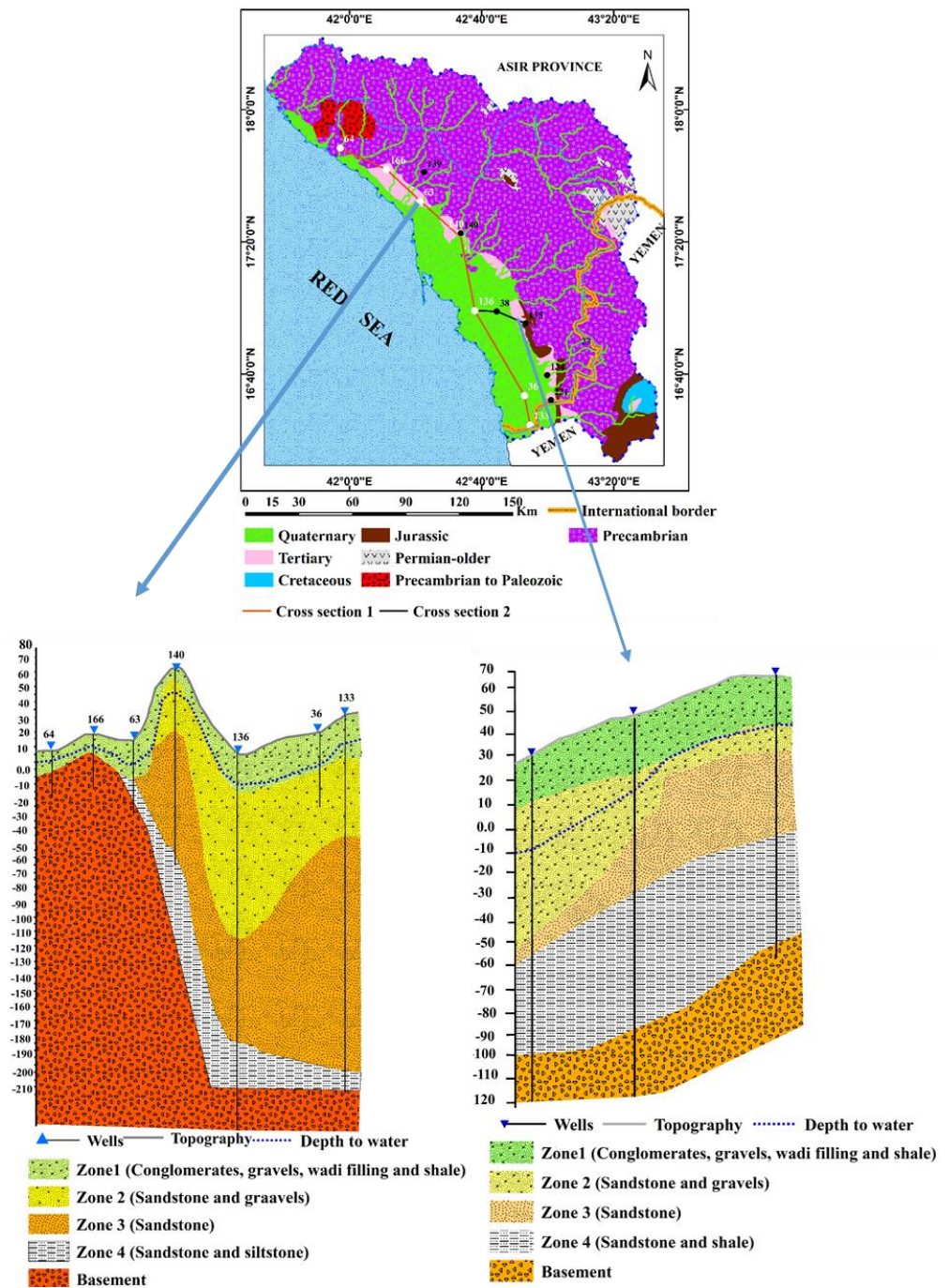
Figure 3. Hydrogeological cross-sections of the study area (unconfined aquifer).

3. Material and Methods

Groundwater Sampling and Analysis

Extensive field works were carried out to identify the representative groundwater sampling wells in the study area. Eighty groundwater samples were collected in pre-cleaned HDPE bottles and stored at 4 °C. In the field, electrical conductivity (EC) and pH were measured by a portable pH/EC meter (SevenGo Duo SG23, Mettler Toledo, Columbus, Ohio, United States). Groundwater samples were analyzed for major and minor ions [33–35]. Groundwater sample analyses were performed in the hydrogeochemistry department and the central laboratory of the Desert Research Centre, based on the methods adopted by [30–32]. Carbonates and bicarbonates were determined by volumetric titrations. The major ions (SO_4^{2-}, Cl^-, Ca^{2+}, Mg^{2+}, Na^+, and K^+) were measured using ion chromatography (Dionex, ICS-1100 Reagent-Free IC System, Sunnyvale, CA, USA). The ion balance error is less than 5%.

Trace elements (Al, B, Cd, Co, Cr, Cu, Fe, Mo, Mn, Ni, Pb, Sr, V, and Zn) were analyzed by ICP-AES (Thermo 6500, Thermo Jarrell elemental company USA). Stock standard solutions (1000 mg/L, Merck) were diluted and prepared various concentrations to calibrate the instrument. To ensure the data quality, blank and known concentration solutions were incorporated into the sample series.

In addition to the 80 samples, 30 representative samples were collected and analyzed for the stable isotopes Oxygen-18 ($\delta^{18}O$) and Deuterium (δD), using PICARRO L2130-i high precision isotopic analyzer. The isotopic compositions are expressed as the difference between the measured ratios of the sample and the VSMOW-reference (Vienna Standard Mean Ocean Water) value divided by the measured ratio of the used reference. Results are presented as per mil deviations from SMOW (δ notation).

4. Results and Discussions

Groundwater in the study site is slightly acidic to neutral in nature and the pH varies from 6.3 to 7.6. The electrical conductivity (EC) and TDS are between 1082 and 23,840 µS/cm and 692 and 15,258 mg/L, reflecting the wide range of chemical signatures between fresh and salt water. Both EC and TDS are increasing from the watershed boundary (Eastern side) towards the Red Sea Coast (Western side). The dominant cations and anions are in the order of $Na^+ > Ca^{2+} > Mg^{2+} > K^+$ and $Cl^- > SO_4^{2-} > HCO_3^- > NO_3^-$, respectively.

4.1. Geochemical Evolution and Flow Path Modeling

According to [36], saturation indices are calculated to recognize the phases of minerals and to detect the geochemical reactions, which are governing the water chemistry as well as assessing the level of equilibrium between water and minerals using PHREEQC code. Reference [37] reported that a saturation index is an approach used to forecast the reacted minerals of the aquifer from groundwater analysis without collecting the samples of the water-bearing formation.

WATEQFP contained in the NETPATHXL 2.0 software [38] is used to compute the ion activity and saturation indices of minerals alongside the flow pathway in the aquifer system.

The degree of saturation can detect if the solution has a thermodynamic possibility for more dissolution or precipitation of minerals. The saturation indices of relevant minerals (SI) were calculated by Equation (1):

$$SI = Log\ (IAP/KT) \tag{1}$$

where IAP is the ion activity product, and KT is the solubility product of the minerals. If the SI = 0, there is an equilibrium between the mineral and the solution; SI < 0 reflects the undersaturation of minerals and possibility for more dissolution whereas SI > 0 indicates super-saturation and precipitation of minerals [5].

The saturation indices of minerals are tabulated in Table 1.

Table 1. Saturation indices values of the groundwater samples in the study area.

Well No	Calcite	Aragonite	Dolomite	Strontianite	Gypsum	Anhydrite	Celestite	SiO$_2$	Sepiolite
1	−0.65	−0.80	−1.56	−2.23	−0.73	−0.96	−1.08	−0.34	−5.69
2	−0.58	−0.73	−1.52	−2.26	−1.14	−1.37	−1.59	−0.50	−5.80
3	−0.56	−0.70	−1.41	−1.26	−0.74	−0.98	−0.22	−1.99	−10.23
4	−0.98	−1.13	−2.18	−2.66	−0.74	−0.98	−1.20	−0.72	−6.81
5	−0.52	−0.67	−1.12	−1.93	−0.96	−1.20	−1.14	−0.30	−4.24
6	−0.72	−0.87	−1.46	−1.95	−0.90	−1.14	−0.90	−0.37	−4.85
7	−0.48	−0.63	−1.07	−1.88	−0.37	−0.60	−0.54	−0.35	−4.10
8	−0.35	−0.50	−0.83	−1.73	−0.27	−0.51	−0.42	−0.38	−4.00
9	−0.31	−0.46	−0.75	−1.80	−0.32	−0.55	−0.58	−0.32	−4.24
10	−0.15	−0.30	−0.54	−1.58	−0.25	−0.49	−0.45	−0.35	−3.62
11	−0.21	−0.35	−0.49	−1.51	−1.27	−1.51	−1.35	−0.32	−3.67
12	−0.24	−0.38	−0.62	−1.70	−1.56	−1.80	−1.79	−0.27	−3.25
13	−0.02	−0.17	−0.26	−1.39	−0.19	−0.43	−0.34	−0.28	−3.65
14	0.10	−0.05	−0.15	−1.33	−0.87	−1.11	−1.06	−0.24	−2.72
15	−0.16	−0.31	−0.51	−1.58	−0.91	−1.14	−1.11	−0.29	−3.94
16	−0.17	−0.32	−0.58	−1.59	−1.15	−1.39	−1.35	−0.17	−4.34
17	−0.42	−0.57	−1.10	−1.84	−1.21	−1.45	−1.40	−0.34	−4.78
18	−0.42	−0.57	−1.09	−1.73	−0.49	−0.72	−0.56	−0.40	−4.87
19	−0.17	−0.32	−0.59	−1.54	−0.89	−1.13	−1.03	−0.28	−3.28
20	−0.21	−0.35	−0.46	−1.56	−0.30	−0.53	−0.43	−0.36	−3.41
21	−0.40	−0.55	−0.90	−2.31	0.09	−0.15	−0.58	−0.37	−4.79
22	0.00	−0.15	−0.01	−3.00	0.16	−0.07	−1.60	−1.59	−6.80
23	−0.10	−0.24	−0.17	−1.73	−0.35	−0.59	−0.75	−0.76	−3.70
24	−0.30	−0.45	−0.79	−2.21	−0.72	−0.95	−1.41	−0.70	−5.36
25	−0.33	−0.47	−0.84	−2.12	−0.81	−1.05	−1.38	−0.64	−4.96
26	−0.28	−0.42	−0.63	−1.71	−0.85	−1.08	−1.05	−0.46	−3.84
27	−0.17	−0.31	−0.47	−1.59	−1.01	−1.25	−1.20	−0.35	−3.18
28	−0.04	−0.19	−0.19	−1.61	−0.84	−1.07	−1.18	−0.38	−2.70
29	0.09	−0.05	0.10	−1.27	0.05	−0.18	−0.09	−0.39	−2.47
30	0.05	−0.10	−0.09	−1.23	−0.53	−0.76	−0.58	−0.47	−2.97
31	0.01	−0.14	−0.35	−1.42	−0.25	−0.48	−0.45	−0.38	−2.95
32	−0.09	−0.24	−0.51	−0.97	−0.43	−0.66	−0.08	−0.22	−2.26
33	−0.12	−0.27	−0.42	−1.48	−0.29	−0.53	−0.42	−0.33	−2.27
34	0.06	−0.09	−0.09	−1.53	0.14	−0.10	−0.22	−0.57	−3.22
35	0.05	−0.10	0.15	−1.61	−0.06	−0.30	−0.50	−0.64	−2.49
36	0.06	−0.09	0.10	−2.09	−0.21	−0.45	−1.13	−1.00	−3.63

Table 1. *Cont.*

Well No	Calcite	Aragonite	Dolomite	Strontianite	Gypsum	Anhydrite	Celestite	SiO₂	Sepiolite
37	0.07	−0.08	−0.07	−2.85	−0.01	−0.25	−1.71	−1.55	−5.88
38	0.16	0.01	0.12	−2.68	−0.45	−0.69	−2.06	−1.21	−4.40
39	0.14	−0.01	0.10	−3.32	−0.37	−0.60	−2.60	−1.47	−5.19
40	0.14	0.00	0.12	−1.19	−0.41	−0.65	−0.52	−0.32	−1.73
41	−0.15	−0.30	−0.69	−1.56	−0.60	−0.83	−0.78	−0.34	−3.40
42	0.15	0.01	−0.09	−1.29	−0.56	−0.80	−0.78	−0.25	−3.07
43	−0.15	−0.30	−0.45	−1.50	−0.72	−0.96	−0.84	−0.26	−2.78
44	0.16	0.01	−0.03	−1.33	−0.28	−0.52	−0.55	−0.16	−1.93
45	0.06	−0.09	−0.03	−1.29	−0.27	−0.50	−0.39	−0.33	−2.18
46	−0.03	−0.18	−0.38	−0.78	−0.54	−0.78	−0.07	−0.32	−2.65
47	−0.02	−0.17	−0.32	−1.30	−0.36	−0.60	−0.41	−0.32	−2.41
48	−0.07	−0.22	−0.25	−1.32	−0.49	−0.72	−0.51	−0.36	−2.10
49	−0.12	−0.27	−0.38	−1.35	−0.79	−1.02	−0.79	−0.35	−2.04
50	−0.04	−0.19	−0.27	−1.36	−0.28	−0.52	−0.38	−0.37	−2.07
51	0.19	0.04	0.13	−1.11	−0.76	−1.00	−0.83	−0.34	−1.22
52	0.05	−0.10	−0.24	−1.21	−0.22	−0.46	−0.25	−0.33	−2.12
53	0.27	0.12	0.17	−1.15	−0.46	−0.69	−0.64	−0.39	−2.11
54	−0.33	−0.48	−0.78	−1.83	−1.12	−1.35	−1.39	−0.36	−3.03
55	−0.02	−0.17	−0.28	−1.49	−1.15	−1.39	−1.39	−0.36	−2.24
56	0.14	−0.01	−0.07	−1.33	−0.80	−1.04	−1.05	−0.32	−2.19
57	0.09	−0.06	0.05	−1.15	−0.75	−0.99	−0.76	−0.29	−2.10
58	0.28	0.13	0.35	−1.16	−0.50	−0.74	−0.71	−0.31	−1.79
59	0.21	0.06	0.35	−1.01	−0.95	−1.18	−0.93	−0.24	−1.75
60	0.31	0.16	0.52	−1.16	−0.58	−0.81	−0.82	−0.27	−1.19
61	0.29	0.14	0.41	−1.12	−0.54	−0.77	−0.72	−0.35	−1.49
62	0.27	0.13	0.37	−1.12	−0.82	−1.06	−0.99	−0.43	−1.49
63	0.10	−0.05	0.15	−1.16	−0.25	−0.49	−0.29	−0.37	−1.72
64	0.20	0.05	0.33	−1.19	−0.35	−0.59	−0.52	−0.39	−1.88
65	0.33	0.18	0.66	−1.02	0.10	−0.13	−0.01	−0.41	−1.81
66	0.03	−0.11	0.01	−0.59	−0.57	−0.80	0.04	−0.37	−1.59
67	0.07	−0.07	0.07	−1.26	−0.63	−0.87	−0.74	−0.33	−1.59
68	0.21	0.07	0.17	−1.57	−0.67	−0.91	−1.22	−0.49	−2.41
69	0.25	0.11	0.25	−1.46	−0.65	−0.88	−1.14	−0.66	−3.69
70	0.21	0.07	0.26	−1.21	−0.31	−0.55	−0.51	−0.31	−1.45
71	0.10	−0.05	0.14	−0.55	−0.50	−0.74	0.08	−0.31	−1.50
72	0.33	0.18	0.64	−1.09	−0.12	−0.35	−0.30	−0.37	−1.77

Table 1. *Cont.*

Well No	Calcite	Aragonite	Dolomite	Strontianite	Gypsum	Anhydrite	Celestite	SiO$_2$	Sepiolite
73	0.12	−0.03	0.13	−1.36	−1.45	−1.68	−1.70	−0.34	−1.24
74	−0.07	−0.22	−0.24	−1.50	−1.25	−1.48	−1.46	−0.30	−1.67
75	0.17	0.02	0.08	−1.38	−0.43	−0.67	−0.75	−0.35	−2.18
76	0.47	0.32	0.79	−1.04	−0.14	−0.38	−0.42	−0.30	−1.60
77	0.28	0.13	0.36	−1.19	−1.04	−1.27	−1.28	−0.30	−1.36
78	0.43	0.28	0.62	−1.21	−0.48	−0.72	−0.90	−0.36	−1.62
79	0.06	−0.09	0.17	−1.35	−0.39	−0.62	−0.57	−0.18	−1.24
80	0.20	0.05	0.43	−1.17	−1.36	−1.60	−1.51	−0.23	−0.93

The study of the ion activity and saturation indices for different minerals can be summarized and interpreted as follow:

In total, 49% of the groundwater samples are undersaturated with respect to calcite mineral (SI < 1), 74% are undersaturated with respect to aragonite mineral and 61% are undersaturated with respect to dolomite mineral, while the rest of the groundwater samples (51%, 39%, and 26%) show saturation with respect to calcite, dolomite, and aragonite minerals (SI > 1), respectively.

The saturation indices of gypsum, anhydrite, silica, strontionite, and sepiolite minerals show negative values in all of the groundwater samples, indicating undersaturation and there is a possibility for more dissolution of such minerals. Dilution by rainfall is the primary reason for such an extensive undersaturation state regarding the dominant mineral stages in the water-bearing formation.

4.2. Geochemical Evolution and Mixing Ratios Calculations

Geochemical modelling and environmental isotopes were integrated and applied to study the controlling factors of mixing and the evolution of the groundwater chemistry, in addition to the salinity origin at the location of the groundwater wells. Thirty samples were analyzed for the environmental isotopes (O^{18} and Deuterium). The relationship between O-18 and Deuterium and the relation between the O-18 and chloride were plotted to understand the salinity source at the well locations (Figures 4 and 5).

An evaluation of water-rock interaction and the mineral stages of the water-bearing formations are depending on the potential of groundwater flow paths, O^{18} ‰ data, major-ion chemistry, and the relation between isotope data and major ion concentrations ($\delta^{18}O$ and Cl). According to [5], the presence of chloride in the mixing process is a result of the traceability of chloride and its non-removal from the system because of its high solubility.

Geochemical model for reactions along a flow path NETPATH (version 2.0) [39] was used to understand the net geochemical mass balance reactions between initial and final water along a hydrologic flowing pathway. When two or more initial waters mix and then react, NETPATH calculates the mixing percentage amount of the two to five initial waters and net geochemical reactions that can explain the composition of the final water by using chemical and isotopic data. Despite the fact that inverse geochemical models do not produce unique results, they do provide results that take into account the observed changes in water chemistry along a flow path, for phases (minerals, salts, or gases) that are known to occur in the aquifers and are usually considered in geochemical analyses.
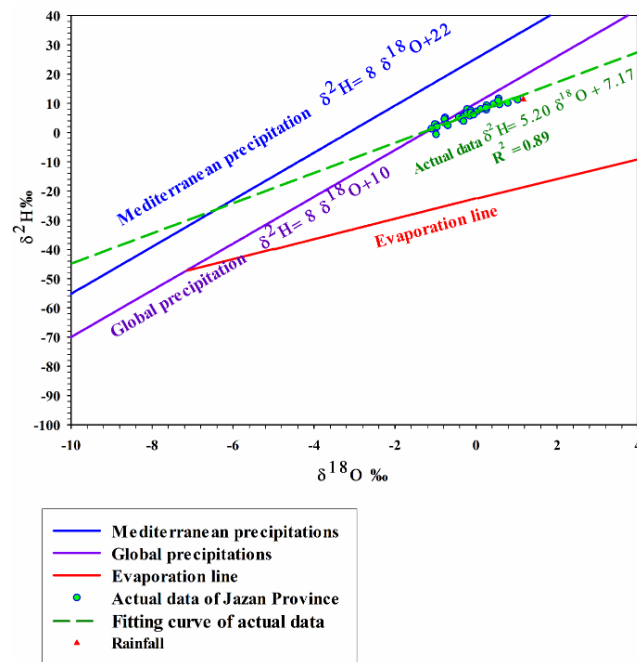
**Figure 4.** Relationship between $\delta^{18}O$ ‰ and $\delta^{2}H$‰.
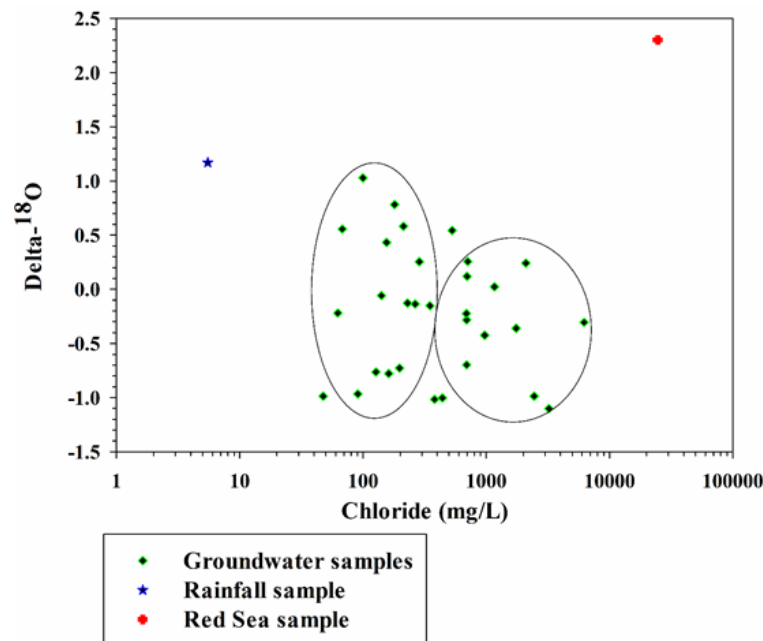
Figure 5. Relationship between Cl and $\delta^{18}O$ values of water samples.

In this study, the water-rock reaction models were constrained by the concentration of major ions (calcium, magnesium, potassium, sodium, chloride, sulphate, and carbonate) of all the selected groundwater samples, in addition to reference waters, such as rain and sea waters. Halite, calcite, montmorillonite, cation exchange, gypsum, dolomite silica, strontionite, and sepiolite minerals were included as phases in NETPATH models due to the alluvial plain deposits (sand mixed with silt and dark clay) that cover most parts of the study area.

Differentiation between the computed models is made by comparing the state of the prevailing minerals in each model (whether they are dissolved or precipitated) with those that were calculated using the WATEQ program. Reference [40] reported that to be

considered valid, simulations of water-rock reaction must not exceed 15 millimoles per liter (mmol/L) precipitation or dissolution of any phase along the proposed flowing pathway.

Three evolutionary paths were chosen along the groundwater flow direction from upstream to downstream (Figure 6). The mineralogical evolution of sample no. 69 to sample no. 29 along flowpath-A takes place on account of calcite and dolomite precipitation as well as Ca-mont., sylvite, gypsum, silica, and sepiolite dissolution at the rate of 12.3, 0.17, 15.18, 14.8, and 7.47 mmol/kg H_2O, respectively (Table 2).
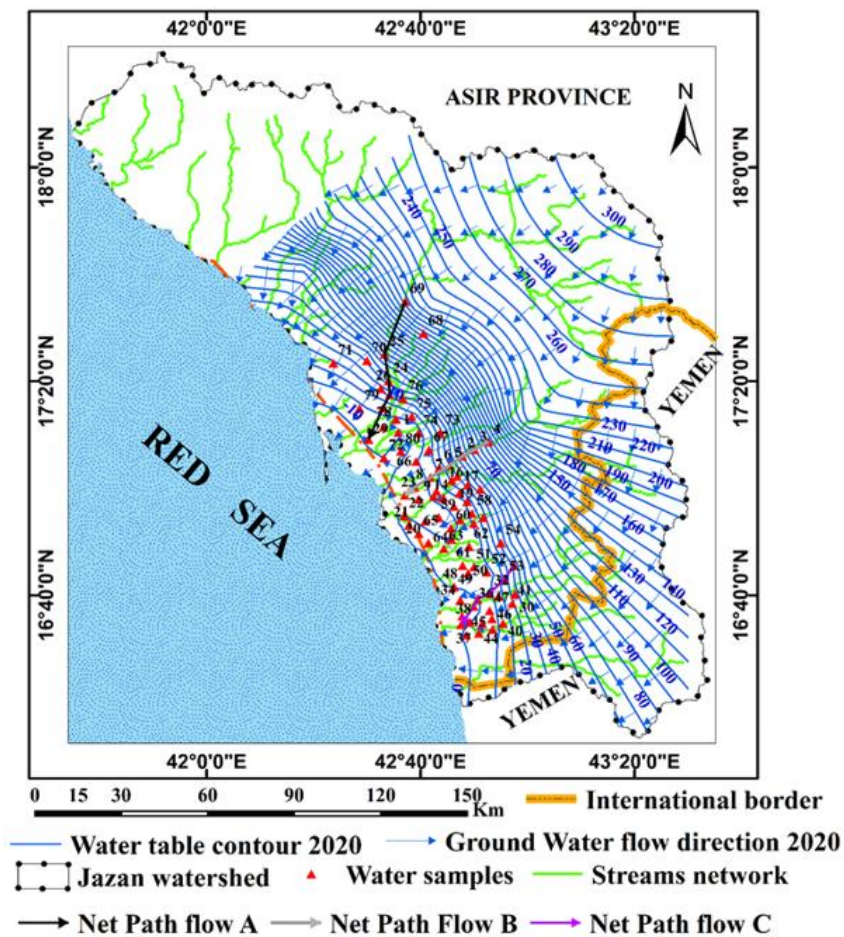

Figure 6. Directions of the evolution for selected flowpaths according to the groundwater flow direction of the water table (interpolation by Kriging method).

Table 2. The mineralogical evolution along the selected flowpaths.

Flowing Pathway A		Flowing Pathway B		Flowing Pathway C	
Minerals Involved (mmol/kg H_2O)		Minerals Involved (mmol/kg H_2O)		Minerals Involved (mmol/kg H_2O)	
CALCITE	−0.75168	CALCITE	−11.63734	CALCITE	−4.40744
Ca−MONT	12.32145	Ca−MONT	0.00566	Ca−MONT	9.09341
SYLVITE	0.16605	SYLVITE	6.22078	SYLVITE	0.35017
DOLOMITE	−1.57484	GYPSUM	10.55809	GYPSUM	14.17006
GYPSUM	15.1858	SEPIOLIT	−0.00004	SiO_2	12.20306
SiO_2	14.80311	CELESTIT	−0.17823	SEPIOLIT	4.3475
SEPIOLIT	7.46899	ALBITE	−0.0185	CELESTIT	−2.43591

Note: negative sign means precipitation, while the positive sign refers to the dissolution.

The chemical dissolution or precipitation is marked based on the saturation index. The dissolved salts are either disseminated within the aquifer matrix or washed out from dry fall constituents. The mineralogical evolution of sample no. 4 to sample no. 23 along the flowpath-B takes place on account of calcite, sepiolite, celestine, and albite precipitation as well as Ca-mont., sylvite, and gypsum dissolution in the rate of 11.64, 0.01, 6.22, 10.56, 0.00, 0.18, and 0.02 mmol/kg. H_2O, respectively (Tables 3 and 4). The mineralogical evolution of sample no. 42 to sample no. 37 along the flowpath-C takes place on account of calcite and celestine precipitation as well as Ca-mont., sylvite, gypsum, silica, and sepiolite dissolution in the rate of 4.41, 9.09, 0.35, 14.17, 12.20, 4.35, 2.44 mmol/kg. H_2O, respectively (Tables 3 and 4).

Table 3. Initial (green color) and final (orange color) chemical composition according to the flow path.

Flow Path	Well No	EC	pH	TDS ppm	Ca	Mg	Na	K	Total Cations	CO₃	HCO₃	SO₄	Cl	Total Anions	SiO₂
										mmoles/L					
Flow path A	69	2467.0	7.1	1533.5	5.48	2.62	7.83	0.45	16.38	0.00	6.63	6.97	5.09	18.70	0.38
	25	1451.0	6.8	1145.0	3.80	2.11	6.09	0.33	12.32	0.00	4.55	5.73	2.82	13.09	0.40
	24	2070.0	6.7	1417.9	4.96	2.73	7.40	0.49	15.57	0.00	4.94	6.25	6.02	17.20	0.35
	77	1408.0	7.5	902.8	2.73	1.48	6.53	0.03	10.76	0.00	4.68	4.06	2.08	10.82	0.89
	27	1779.0	7.1	1136.7	2.40	1.51	10.01	0.10	14.02	0.00	5.20	5.41	2.57	13.18	0.78
	29	12,330.0	6.9	7272.9	23.23	15.87	43.50	0.28	82.88	0.00	3.12	24.98	69.11	97.22	0.68
Flow path B	4	2254.0	6.40	1410.04	4.11	2.16	9.57	0.31	16.16	0.00	2.47	6.77	6.63	15.87	0.33
	3	2002.0	6.50	1201.03	4.72	2.05	5.22	0.40	12.39	0.00	4.29	5.62	4.39	14.30	0.02
	2	1082.0	6.60	656.55	2.75	1.04	3.05	0.22	7.06	0.00	4.42	2.71	1.34	8.47	0.55
	5	1480.0	6.70	927.00	3.01	2.20	4.35	0.24	9.80	0.00	4.29	4.68	1.77	10.74	0.89
	7	3920.0	6.70	2530.48	6.80	4.51	15.23	0.26	26.79	0.00	3.25	15.41	5.90	24.56	0.78
	8	4650.0	6.70	2994.88	8.77	5.78	17.40	0.36	32.32	0.00	3.51	16.66	10.76	30.93	0.72
	23	7660.0	7.00	4689.27	8.68	7.82	34.80	6.50	57.80	0.00	3.51	17.07	38.08	58.67	0.30
Flow path C	42	3070.0	7.0	1996.8	6.37	2.19	14.79	0.20	23.55	0.00	6.24	8.33	9.87	24.44	0.99
	53	3100.0	7.3	1976.0	7.49	2.78	10.44	0.39	21.09	0.00	3.51	9.37	9.77	22.65	0.71
	32	3410.0	7.2	2245.4	5.75	2.37	17.40	0.18	25.70	0.00	2.86	14.16	2.91	19.93	1.05
	33	5130.0	7.1	3258.1	9.36	5.40	20.45	1.78	36.97	0.00	2.21	15.09	19.61	36.91	0.81
	36	6030.0	7.2	4191.8	9.98	8.23	28.71	0.82	47.74	0.00	2.86	20.82	22.92	46.60	0.17
	37	13,110.0	7.0	7630.3	20.51	10.80	62.64	0.55	94.50	0.00	2.60	22.90	79.13	104.63	0.05
Rain		87	6.94	29.15	0.18	0.02	0.10	0.00	0.30	0.00	0.24	0.07	0.16	0.46	0.00
Sea		67,900	7.80	43,062.71	12.48	80.98	542.88	9.21	645.54	0.42	2.10	31.23	695.81	729.55	0.00

Table 4. Netpath mixing ratio calculations in some selected groundwater samples.

Final Water	Mixing (Percent)				
	Initial 1 Well 2	Initial 2 Well 4	Initial 3 Well 7	Initial 4 Rain	Initial 5 Sea
17	–	79%	–	21%	0.00%
21	–	23%	–	7%	70%
23	14%	0.00%	77%	5%	4%
55	–	45%	–	53%	2%
65	–	50%	–	32%	18%
72	–	37%	–	26%	37%
73	–	64%	–	36%	0.00%
80	–	65%	–	34%	0.00%

The calculation of the mixing ratios of three reference waters known as initial waters (well no. 4, rain, and sea) in samples no. 17, 21, 55, 65, 72, 73, and 80, as shown in Figure 7, were computed based on Cl and/or δO^{18}. On the other hand, the ratio of five initials (wells no. 2, 4, 7, rain, and sea) was computed in sample no. 23, (Tables 3 and 4).
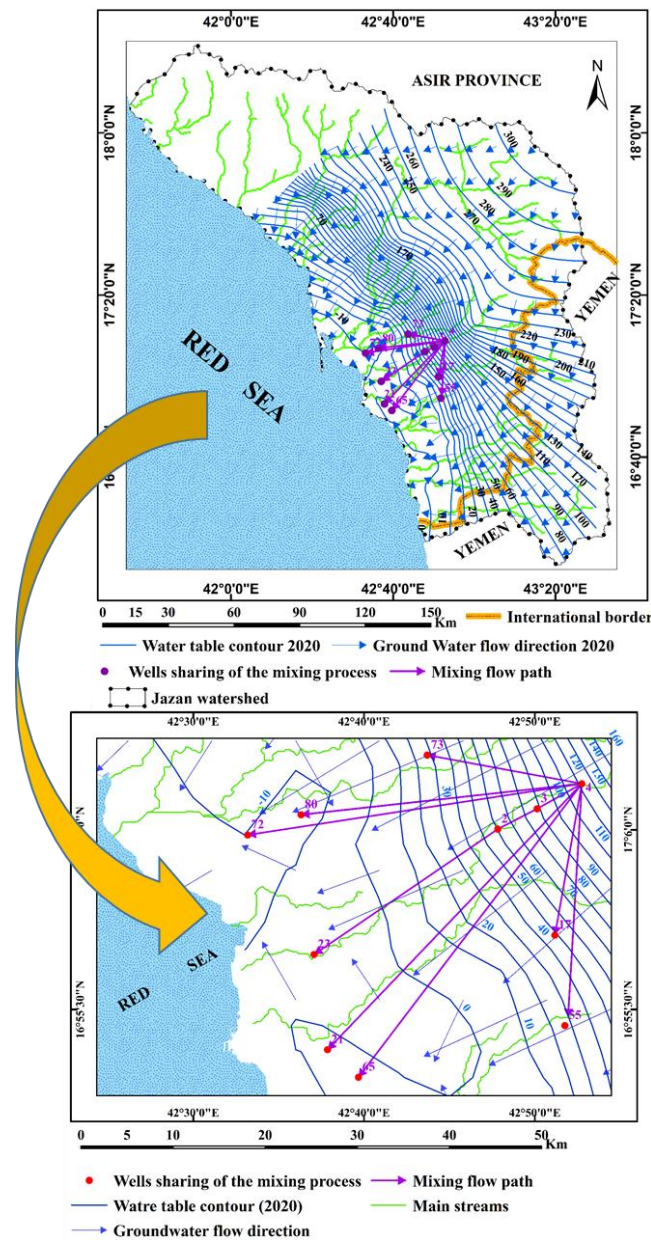
**Figure 7.** Mixing ratios of three reference waters known as initial waters or (4, rain, and sea) in samples (17, 21, 55, 65, 72, 7,3, and 80) as final waters.

The resulting mixing models computed by NETPATH (based on chloride) revealed the composition of sample no. 17 was modified from initials 4, rain, and sea as a result of mixing of such samples in the ratio of 79%, 21%, and 0%, respectively. Likewise, the composition of sample no. 21 was modified from initials 4, rain, and sea as a result of mixing of such samples in the ratio of 23%, 7%, and 70%, respectively. Similarly, the composition of sample no. 23 is modified from initials 2, 4, 7, rain, and sea as a result of the mixing of such samples in the ratio of 14%, 0%, 77%, 5%, and 4%, respectively. The composition of sample no. 55 was modified from initials well no. 4, rain, and sea as a result of mixing of such samples in the ratio of 45%, 53%, and 2%, respectively. The composition

of sample no. 65 was modified from initials well no. 4, rain, and sea as a result of the mixing of such samples in the ratio of 50%, 32%, and 18%, respectively. The composition of sample no. 72 was modified from initials well no. 4, rain, and sea as a result of mixing of such samples in the ratio of 37%, 26%, and 37%, respectively. Finally, the composition of sample no. 73 and 80 modified from initials well no. 4, rain and sea showed the same contribution from initial waters with the ratio of 64%, 36%, and 0%, respectively.

4.3. Sources of Salinity in Groundwater

Seawater or evaporites are the major sources of salinity in the coastal shallow aquifer. In a water-bearing formation, environmental isotopes are preserved much better than other components, which may undergo ion exchange processes or precipitation processes. The dissolution and flushing of dry salt by precipitation and other meteoric water will not affect environmental isotope conservation [41–43]. The influence of seawater (seawater intrusion) on the coastal belt is clearly noticed on well no. 21, 65, and 72; however, it shows less or no effect on wells 23, 55, 17, 73, and 80. Furthermore, there is a variable contribution of rainwater in all of the selected groundwater samples. The results of the environmental isotopes (Figures 4 and 5) show that the water samples are close to the global precipitation line with a correlation coefficient (r^2) of the fitting line at 0.89 and this fitting line is parallel to the evaporation line (Figure 4). This means that the source of the study groundwater is of meteoric (global precipitation) origin and is influenced by the evaporation process before recharging the groundwater aquifer.

The relationship between the $\delta^{18}O$ and chloride (salinity) is shown in Figure 5. Figure 5 illustrates two groups of samples and salinity increases with decreasing δO^{18}. Generally, groundwater samples with less saline (Cl < 500 mg/L) fall into Group A. Group A samples are most likely affected by rainfall recharge and seem to be recent water. However, samples accumulated in Group B are predominantly affected by the evaporation process followed by the dissolution of minerals.

5. Conclusions and Recommendations

The geochemical flow path model is generally very important to evaluate and predict the geochemical processes in groundwater flow directions. The objectives of this research are to understand and explain the hydrochemical factors which are governing the chemical composition of groundwater in the shallow groundwater systems and to identify the predominant processes in the groundwater flow direction. Geochemical modelling and environmental isotopes were integrated and applied to study the controlling factors of mixing and evolution, in addition to the salinity origin of the study groundwater wells. The major cations and anions are in the order of $Na^+ > Ca^{2+} > Mg^{2+} > K^+$ and $SO_4^{2-} > HCO_3^- > NO_3^-$, respectively. A geochemical model, NETPATH, was used to recognize the hydrochemical processes in the groundwater resource in the study area by three flow pathways A, B, and C. In all, 49% of the groundwater samples are undersaturated with respect to calcite mineral (SI < 1), 74% are undersaturated with respect to aragonite mineral, and 61% are undersaturated with respect to dolomite mineral; meanwhile, the remaining groundwater samples (51%, 39%, and 26%) are saturated in terms of calcite, dolomite and aragonite minerals (SI > 1), respectively. The saturation indices of gypsum, anhydrite, silica, strontionite, and sepiolite minerals, show negative values in all of the groundwater samples, indicating undersaturation and a high potential for the dissolution of such minerals. Dilution by rainfall is the primary reason for such an extensive undersaturation state regarding the dominant mineral stages in the water-bearing formation. The chemical dissolution or precipitation is marked based on the saturation index. The dissolved salts are either disseminated within the aquifer matrix or washed out from dry fall constituents. The influence of seawater (seawater intrusion) on groundwater clearly appeared on well no. 21, 65, and 72, but it is not noticed on wells 23, 55, 17, 73, and 80 in the coastal region. The relationship between $\delta^{18}O$ and δD shows clearly that the studied shallow groundwater

aquifer is affected by surface runoff recharge, as well as evaporation processes, along with mineral dissolution.

References

1. Perri, F.; Scarciglia, F.; Apollaro, C.; Marini, L. Characterization of granitoid profiles in the Sila Massif (Calabria, southern Italy) and reconstruction of weathering processes by mineralogy, chemistry, and reaction path modeling. *J. Soils Sediments* **2014**, *15*, 1351–1372. [CrossRef]

2. Perri, F.; Ietto, F.; Le Pera, E.; Apollaro, C. Weathering processes affecting granitoid profiles of Capo Vaticano (Calabria, southern Italy) based on petrographic, mineralogic and reaction path modelling approaches. *Geol. J.* **2016**, *51*, 368–386. [CrossRef]

3. Rabeiy, R.E. Assessment and modeling of groundwater quality using WQI and GIS in Upper Egypt area. *Environ. Sci. Pollut. Res.* **2017**, *25*, 30808–30817. [CrossRef] [PubMed]

4. Apollaro, C.; Perri, F.; Le Pera, E.; Fuoco, I.; Critelli, T. Chemical and minero-petrographical changes on granulite rocks affected by weathering processes. *Front. Earth Sci.* **2019**, *13*, 247–261. [CrossRef]

5. Appelo, A.; Postma, D. *Geochemistry, Groundwater and Pollution*, 2nd ed.; Balkama: Rotterdam, The Netherlands, 2005; Volume 536. [CrossRef]

6. El Osta, M.; Masoud, M.; Ezzeldin, H. Assessment of the geochemical evolution of groundwater quality near the El Kharga Oasis, Egypt using NETPATH and water quality indices. *Environ. Earth Sci.* **2020**, *79*, 56. [CrossRef]

7. Dhakate, R.; Ratnalu, G.V.; Sankaran, S. Hydrogeochemical and isotopic study for evaluation of seawater intrusion into shallow coastal aquifers of Udupi District, Karnataka, India. *Geochemistry* **2020**, *80*, 125647. [CrossRef]

8. Rajmohan, N.; Elango, L. Hydrogeochemistry and its relation to groundwater level fluctuation in the Palar and Cheyyar river basins, southern India. *Hydrol. Process.* **2006**, *20*, 2415–2427. [CrossRef]

9. Rajmohan, N.; Prathapar, S.A. Assessment of geochemical processes in the unconfined and confined aquifers in the Eastern Ganges Basin: A geochemical approach. *Environ. Earth Sci.* **2016**, *75*, 1212. [CrossRef]

10. Manikandan, E.; Rajmohan, N.; Anbazhagan, S. Monsoon impact on groundwater chemistry and geochemical processes in the shallow hard rock aquifer. *CATENA* **2020**, *195*, 104766. [CrossRef]

11. Rajmohan, N.; Masoud, M.H.; Niyazi, B.A. Impact of evaporation on groundwater salinity in the arid coastal aquifer, Western Saudi Arabia. *CATENA* **2021**, *196*, 104864. [CrossRef]

12. Elango, L.; Kannan, R. Rock–water interaction and its control on chemical composition of groundwater. In *Concepts and Applications in Environmental Geochemistry*; Elsevier: Amsterdam, The Netherlands, 2007; Volume 5, Chapter 11; pp. 229–243.

13. AbdelRahman, M.A.; Shalaby, A.; Mohamed, E. Comparison of two soil quality indices using two methods based on geographic information system. *Egypt. J. Remote Sens. Space Sci.* **2019**, *22*, 127–136. [CrossRef]

14. Elbeih, S.F.; Madani, A.A.; Hagage, M. Groundwater deterioration in Akhmim District, Upper Egypt: A Remote Sensing and GIS investigation approach. *Egypt. J. Remote Sens. Space Sci.* **2021**, *24*, 919–932. [CrossRef]

15. El-Zeiny, A.M.; El-Hamid, H.T.A. Environmental and human risk assessment of heavy metals at northern Nile Delta region using geostatistical analyses. *Egypt. J. Remote Sens. Space Sci.* **2022**, *25*, 21–35. [CrossRef]

16. Abdalla, F. Ionic ratios as tracers to assess seawater intrusion and to identify salinity sources in Jazan coastal aquifer, Saudi Arabia. *Arab. J. Geosci.* **2015**, *9*, 40. [CrossRef]

17. Masoud, M.H.Z.; Basahi, J.M.; Rajmohan, N. Impact of flash flood recharge on groundwater quality and its suitability in the Wadi Baysh Basin, Western Saudi Arabia: An integrated approach. *Environ. Earth Sci.* **2018**, *77*, 395. [CrossRef]

18. Masoud, M.H.Z.; Basahi, J.M.; Zaidi, F.K. Assessment of artificial groundwater recharge potential through estimation of permeability values from infiltration and aquifer tests in unconsolidated alluvial formations in coastal areas. *Environ. Monit. Assess.* **2019**, *191*, 31. [CrossRef] [PubMed]

19. Rajmohan, N.; Niazi, B.A.M.; Masoud, M.H.Z. Evaluation of a brackish groundwater resource in the Wadi Al-Lusub basin, Western Saudi Arabia. *Environ. Earth Sci.* **2019**, *78*, 451. [CrossRef]

20. Zaigham, N.A.; Aburizaiza, O.S.; Mahar, G.A.; Nayyar, Z.A. Hydrogeologic assessment for groundwater prospects in Al-Abwa drainage basin, arid-terrain of Arabian Shield, Saudi Arabian Red Sea coastal belt. *Arab. J. Geosci.* **2020**, *13*, 370. [CrossRef]

21. Rajmohan, N.; Masoud, M.H.Z.; Niyazi, B.A.M. Assessment of groundwater quality and associated health risk in the arid environment, Western Saudi Arabia. *Environ. Sci. Pollut. Res.* **2021**, *28*, 9628–9646. [CrossRef]

22. Plummer, L.N. Geochemical modelling of water–rock interaction: Past, present, future. *Proc. Int. Symp. Water–Rock Interact.* **1992**, *7*, 23–33.

23. Kumar, A.; Rout, S.; Narayanan, U.; Manish, K.; Mishra, R.; Tripathi, M.; Singh, J.; Kumar, S.; Kushwaha, H.S. Geochemical modelling of uranium speciation in the subsurface aquatic environment of Punjab state in India. *J. Geol. Min. Res.* **2011**, *3*, 137–146.

24. Trabelsi, R.; Zouari, K. Coupled geochemical modeling and multivariate statistical analysis approach for the assessment of groundwater quality in irrigated areas: A study from North Eastern of Tunisia. *Groundw. Sustain. Dev.* **2019**, *8*, 413–427. [CrossRef]

25. Garrels, R.M.; Thompson, M.E. A chemical model for sea water at 25 °C and one atmosphere total pressure. *Amer. J. Sci. 1962 260*, 57–66. [CrossRef]

26. Sun, L.H.; Gui, H.R. Establishment of water source discrimination model in coal mine by using hydrogeochemistry and statistical analysis: A case study from Renlou Coal Mine in northern Anhui Province, China. *J. Coal. Sci. Eng.* **2012**, *18*, 385–389. [CrossRef]

27. Sklash, M.G.; Farvolden, R.N. The Role of Groundwater in Storm Runoff. *J. Hydrol.* **1979**, *43*, 45–65. [CrossRef]

28. Gui, J.; Li, Z.; Yuan, R.; Xue, J. Hydrograph separation and the influence from climate warming on runoff in the north-eastern Tibetan Plateau. *Quat. Int.* **2019**, *525*, 45–53. [CrossRef]

29. Xia, C.; Liu, G.; Xia, H.; Jiang, F.; Meng, Y. Influence of saline intrusion on the wetland ecosystem revealed by isotopic and hydrochemical indicators in the Yellow River Delta, China. *Ecol. Indic.* **2021**, *133*, 108422. [CrossRef]

30. Falcone, R.A.; Falgiani, A.; Parisse, B.; Petitta, M.; Spizzico, M.; Tallini, M. Chemical and isotopic (δ18O‰, δ2H‰, δ13C‰, 222Rn)multi-tracing for groundwater conceptual model of carbonate aquifer(Gran Sasso INFN underground laboratory–central Italy). *J. Hydrol.* **2008**, *357*, 368–388. [CrossRef]

31. Medici, G.; Langman, J.B. Pathways and Estimate of Aquifer Recharge in a Flood Basalt Terrain; A Review from the South Fork Palouse River Basin (Columbia River Plateau, USA). *Sustainability* **2022**, *14*, 11349. [CrossRef]

32. Jeelani, G.; Lone, S.A.; Nisa, A.U.; Deshpande, R.D.; Padhya, V. Use of stable water isotopes to identify and estimate the sources of groundwater recharge in an alluvial aquifer of Upper Jhelum Basin (UJB), western Himalayas. *Hydrol. Sci. J.* **2021**, *66*, 2330–2339. [CrossRef]

33. Rainwater, F.H.; Thatcher, L.L. *Methods for Collection and Analysis of Water Samples*; US Government Printing Office: Washington, DC, USA, 1960. [CrossRef]

34. Fishman, J.; Friedman, C. *Methods for Determination of Inorganic Substances in Water and Fluvial Sediments*; U.S. Geol. Surv. Book 5, Chapter A1; Open-File Report 85-495; USGS: Denver, CO, USA, 1985; Volume 84.

35. American Society for Testing and Materials (A.S.T.M.). Water and Environmental technology. In *Annual Book of ASTM*; Standards, U.S.A. Sec. 11, Vol. 11.01, and 11.02; A.S.T.M.: West Conshohocken, PA, USA, 2002.

36. Aghazadeh, N.; Mogaddam, A. Assessment of groundwater quality and its suitability for drinking and agricultural uses in the Oshnavieh area, Northwest of Iran. *J. Environ. Prot.* **2010**, *1*, 30–40. [CrossRef]

37. Deutsch, J. *Groundwater Geochemistry: Fundamentals and Applications to Contamination*; Lewis Publishers: New York, NY, USA, 1997.

38. Plummer, L.N.; Prestemon, E.C.; Parkhurst, D.L. *An Interactive Code (NETPATH) for Modeling NET Geochemical Reactions along a Flow Path*; U.S. Geological Survey, Water-Resources Investigations Report 91-4078; U.S. Geological Survey: Reston, Virginia, USA, 1991; 227p. [CrossRef]

39. Plummer, L.N.; Prestemon, E.C.; Parkhurst, D.L. *An Interactive Code (NETPATH) for Modeling NET Geochemical Reactions along a Flow Path, Version 2.0*; U.S. Geological Survey Water-Resources Investigations Report 94-4169; U.S. Geological Survey: Reston, Virginia, USA, 1994; 130p. [CrossRef]

40. Hershey, L.; Heilweil, M.; Gardner, P.; Lyles, B.; Earman, S.; Thomas, J.; Lundmark, W. *Ground-Water Chemistry Interpretations Supporting the Basin and Range Regional Carbonate-Rock Aquifer System (BARCAS) Study, Eastern Nevada and Western Utah. DHS*; Publication No. 41230; Desert Research Institute Nevada System of Higher Education: Reno, NV, USA; US. Geological Survey: Reston, VA, USA, 2007.

41. International Atomic Energy Agency (I.A.E.A.). *Stable Isotope Hydrology: Deuterium and Oxygen-18 in the Water Cycle. Monograph Prepared under the Aegis of the I.A.E.A./UNESCO Working Group on Nuclear Techniques in Hydrology of the International Hydrological Program, STI./DOC./10*; I.A.E.A.: Austria, Vienna, 1981; Volume 210.

42. El Osta, M.; Masoud, M.; Alqarawy, A.; Elsayed, S.; Gad, M. Groundwater Suitability for Drinking and Irrigation Using Water Quality Indices and Multivariate Modeling in Makkah Al-Mukarramah Province, Saudi Arabia. *Water* **2022**, *14*, 483. [CrossRef]
43. Alqarawy, A.; El Osta, M.; Masoud, M.; Elsayed, S.; Gad, M. Use of Hyperspectral Reflectance and Water Quality Indices to Assess Groundwater Quality for Drinking in Arid Regions, Saudi Arabia. *Water* **2022**, *14*, 2311. [CrossRef]